IEEE Access
Multidisciplinary ⋮ Rapid Review ⋮ Open Access Journal

Received 10 March 2024, accepted 16 March 2024, date of publication 21 March 2024, date of current version 28 March 2024.

Digital Object Identifier 10.1109/ACCESS.2024.3380353

RESEARCH ARTICLE

A Digital Emulator Design for the Swimming Rhythmic Pattern Generator of a Lamprey

NIMET KORKMAZ
Department of Electrical and Electronics Engineering, Kayseri University, 38280 Kayseri, Turkey
e-mail: nimetkorkmaz@kayseri.edu.tr

This work was supported by the Scientific Research Project Coordination Unit, Kayseri University, under Project FKB-2022-1048.

ABSTRACT It is difficult to perform multiplication with digital devices and required to the more practical implementation methods. Thus, a well-known simpler transfer function adaptation to a swimming pattern generator is suggested for the digital implementation easiness in here. However, the direct adaptation of this function to this neural circuit is insufficient, so a control parameter is included in the laterally inhibitor neurons. Its fittest value is determined by a bifurcation diagram for getting a neural circuit that produces rhythmic patterns. Then, a four-segmented neural swimming pattern generator is constructed by using this simpler function and the anti-phase firings of neuron groups on the opposite sides is observed by the numerical simulations. Additionally, it is aimed to obtain an adjustable time delay between the neural segments, so the 'reciprocal inhibition' synaptic connections are adapted to this four-segmented structure. The effect of the reciprocal inhibition on time delays is observed by the standard deviation and numerical simulations. The final aim is to get the electrical signals with the digital device-based implementation for emulating the swimming rhythmic pattern generator of a lamprey and a **F**ield **P**rogrammable **G**ate **A**rray-based realization is carried out by using the simpler transfer function. To see the achievement of this implementation, the anti-phase firings of neuron groups on the opposite sides and getting an adjustable time delay between neural segments are verified by the electrical signals. Moreover, the swimming pattern generator of a lamprey is realized with FPGA without using any multiplier blocks thanks to the simplification process.

INDEX TERMS Swimming pattern generator, lamprey, reciprocal inhibition, time delay, field programmable gate array (FPGA).

I. INTRODUCTION

The functional mechanism of the brain is the main subject of many researches with different perspectives. Along with this research topic, the rhythmic pattern generator structures have been discovered [1], [2], [3]. These structures are the neural circuits that are the sources of the rhythmic movements such as swimming, locomotion, digestion, heartbeat etc. in the living beings [4], [5]. It is now a known fact that when a certain number of neurons come together with various synaptic connections, they form the neural circuits. These neural circuits produce the rhythmic patterns and they are available in both vertebrates and invertebrates [6], [7], [8]. All neurons and their interactions are modeled in these neural circuits, mathematically. There are many examples of the neural circuit models in the literature and the internal interactions among the neurons are able to be examined with these models, functionally. One of the most widely known of these structures is swimming rhythmic pattern generator of a lamprey (see Fig.1) [9], [10], [11], [12], [13]. Some basic assumptions have been made about the neurons and their interactions in the swimming rhythmic pattern generator of a lamprey. Some of these acceptances are as follows: i) There are reciprocally interacting neuron groups on the right and left sides in the swimming pattern generator of a lamprey, ii) These right and left neuron groups maintain to produce rhythmic patterns within themselves; even they are isolated from each other, iii) These neuron groups are coupled with

The associate editor coordinating the review of this manuscript and approving it for publication was Ludovico Minati.

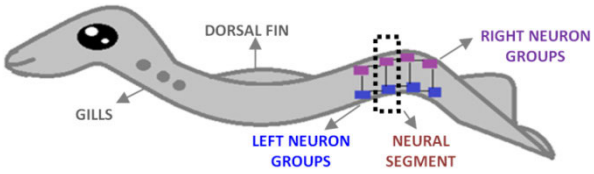

FIGURE 1. A simple representative draft for swimming pattern generator of a lamprey.

each other through along the spinal cord of a lamprey (from head to tail), iv) One excitatory 'EIN', two inhibitory (one of them is laterally inhibitor neuron 'LIN' and another of them is collaterally inhibitor 'CIN' neurons) interneurons and one motor neuron 'M' are available in each neuron groups on the right and left sides, v) Each of these neurons interacts with each other, with the other neurons on the opposite side, and with neighboring neural segments, vi) The neurons on the right and left sides fire in anti-phase. vii) There is a certain time delay between neuron firings in each neural segment, thanks to these time delays, the neural segments triggered sequentially and they create the fluctuating movement in the living being. As seen from these assumptions, the anti-phase firing between the right and left neuron groups and a time delay between neural segments are among the primary requirements for the formation of the swimming pattern of lampreys.

Many studies have been carried out on the models that provide these features mentioned above. One of the most well-known of them is the model proposed by Ekeberg [14], [15]. The neurons act as integrators according to this model. Several delay parameters have been defined to get time delays. The excitatory input has been limited by a function and this boundary function includes an exponential expression. Another model is presented to the literature by Anzinger & Rottoy [16] in 2009 for modeling the swimming pattern generator of a lamprey. Their model is based on the integrated and fire neuron model and describes the average evoked activity of a neuron populations in a neural segment. The model includes a sigmoid-shape transfer function for limiting the output signal.

The next stage of the modeling studies is to develop neuromorphic systems. These neuromorphic systems, which are developed using swimming pattern generator of a lamprey, have several applications in different research areas. For example, an interaction between a real-time circuit and spinal cord of a lamprey has been explored as an neuroprosthetic applications in [17] and a VLSI circuit design has been improved for that generating the spinal motor pattern. In [18], a visually guided robotic lamprey has been designed and the anguilliform swimming of this robot has been controlled by validating output of the computational neuron model. The investigation of the novel telepresence strategies and the validation of the neuroscience models has been handled by designing a neurobotic artificial lamprey model in [19]. The study in [20] has been focused on controlling the locomotion of a lamprey robot and it is demonstrated the adjustment easily the speed and direction of locomotion by the central pattern generator. The dorsal fins affect the swimming speed and performance of the bioinspired underwater robots and a systematic dual dorsal fin design has been performed in [21] for swimming efficiency of a snake-like underwater robot. In these applications, it can be aimed to implement a neuromorphic emulator circuit by utilizing the rhythmic pattern generator models [22], [23], [24]. However, the realizations of the exponential boundary functions in these mentioned models are quite difficult directly with the digital equipment. There are many different approaches to overcome this problem in the literature. Several approaches such as linearization operations [25], [26], integration of different computational methods into the systems [27] and the usage of an approximation functions [28], [29] are suggested for the simplification of the exponential function, so it has been gotten the revised boundary expressions compatible with the digital systems. The fact that both swimming pattern generator models mentioned above also contain exponential expressions and this situation makes difficult their digital equipment-based implementations. In this study, it is aimed to make a simplification in the activation function of the model, which is derived from the integrated and fire type neuron models by Anzinger & Rottoy [16], so it is aimed realization easiness with the digital equipment. In this context, the linear-characterized 'sign' function is adapted to the model instead of the sigmoid-shaped transfer function. Although the 'sign' function has several convergence drawbacks in terms of the signal continuity, it is easier to model mathematically this function instead of an exponential model. It is possible to construct a sigmoid shape function with the analog circuit devices such as voltage comparators and differential amplifiers. In fact, this realization process may be quite suitable for prototype trials. However, the analog circuits have disadvantages such as sensitivity to noise, inflexible designs and inability to hold the previous data. On the other hand, due to the increasing number of neurons in a neural network structure design, the number of the used hardware increases and the connections between the emulated neurons become extremely complex. For this reason, the usage of programmable electronic devices comes forward instead of discrete device-based analog designs in such realizations. Although the neural systems can be designed with programmable analog circuit devices such as Field Programmable Analog Arrays [30], [31], the limited memory problems are encountered in such also devices as the number of neurons in the neural structure increases. Thus, the programmable digital devices prefer in the hardware implementations of the neural systems. The digital circuits are more compatible with existing hardware to develop systems that can meet different requirements in the different situations. For this reason, in this study, the digital device-based application is used for the neuromorphic circuit realization of the swimming rhythmic pattern generator of the lamprey and the **F**ield **P**rogrammable **G**ate **A**rray-FPGA device is preferred in this implementation with its prominent features

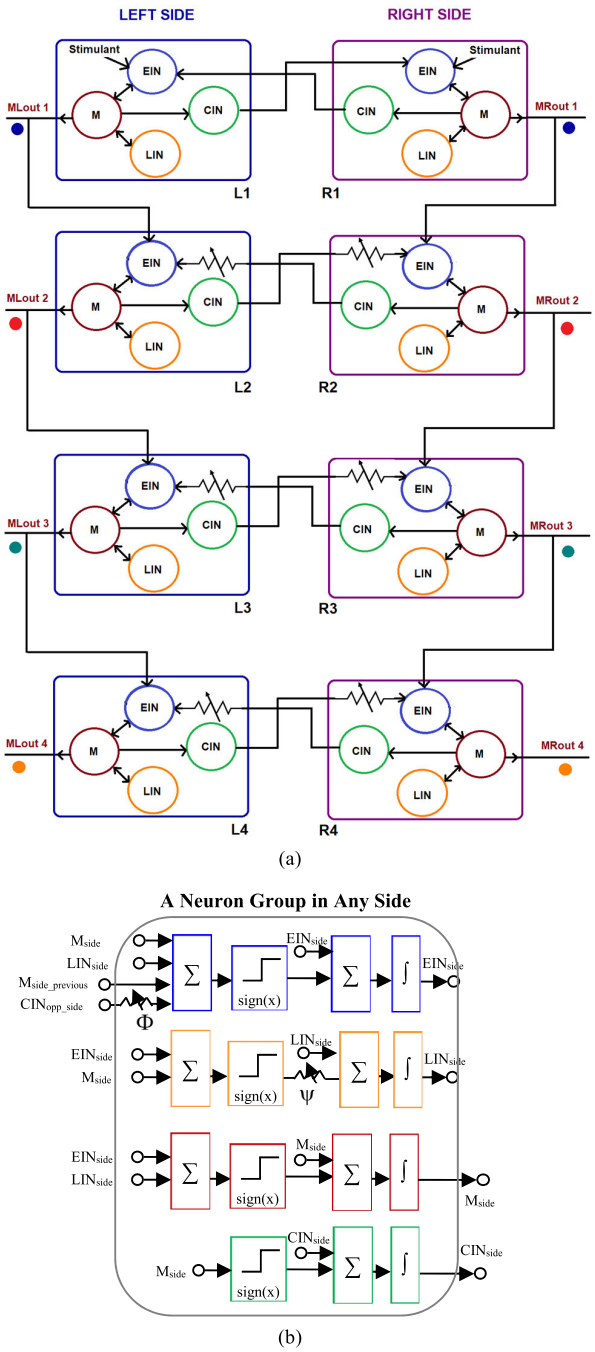

FIGURE 2. a) An extended and updated network design from for the swimming pattern generator of a lamprey [16], b) A representative illustration of a neuron group in mathematical form.

such as parallel programmability and the design system on a chip.

On the other hand, the direct adaptation of the 'sign' function to this model is insufficient to obtain a network structure that produces the rhythmic swimming patterns. Thus, a control parameter 'Ψ' is included in the laterally inhibitor interneuron in the neuron groups and the effect on the swimming network of this control parameter is observed with a bifurcation diagram. After determining an appropriate value of this control parameter, a swimming pattern generator network in [16] is extended and updated as in Fig.2a.

In general, when the studies about central pattern generator structures in the literature are examined, it is stated that 'reciprocal inhibition' is also effective as one of the sources of time delays between neuron firings [8], [32]. From this point of view, it is also aimed to obtain time delays between neural segments by changing the synaptic weights. The collaterally inhibitor interneuron indicated by the 'CIN' are connected to the excitatory interneuron 'EIN' on the opposite side by a variable synaptic weight in each neural segments (see Fig.2). Therefore, in here, i) the results of the anti-phase firings between neuron groups on the right and left sides, ii) results of time delays between neural segments, and iii) the results that show the effect of the reciprocal inhibition connections on the time delays are firstly presented with standard deviation results and numerical simulation studies by using the revised swimming pattern generator model. Then, the final aim of this study is to get the electrical signals for emulating the swimming pattern generator of a lamprey by using digital equipment and the swimming pattern generator network given in Fig.2a is realized by using the '**F**ield **P**rogrammable **G**ate **A**rray-FPGA' device. The FPGA device is one of the hardware that is an alternative device instead of discrete devices and analog systems in the implementations of the central pattern generators [33], [34], [35], [36], [37], [38], [39], [40]. FPGAs are among the pioneer electronic equipment to verify prototype designs; thanks to its programmability feature and parallel working principle. In this study, all numerical simulation results for the designed swimming pattern generator network in Fig.2a are repeated with the electrical signals that are obtained by the FPGA-based implementations. Thus, the proposed simplification and the control processes are accomplished for the swimming rhythmic pattern generator model of a lamprey, successfully and the electrical signals are obtained in an efficient way. We aim the less hardware usage in digital circuits with the simplification process of the boundary function and it is achieved with the use of no multipliers by using a simpler definition instead of the exponential function.

The following parts of this study are organized as follows: After introducing of the swimming pattern generator of a lamprey, its network model definition and the proposed simplifications about this model are given in Section II. The results of the bifurcation diagram that is illustrated the effect of the control parameter on the pattern generation and the aforementioned standard deviation and numerical simulation results are also presented in this section. The realization details of the swimming rhythmic pattern generator with the FPGA device are presented in Section III. The electrical signal measurement results, which are recorded from the neuromorphic swimming pattern generator, are also presented in this section. The synthesis results of the FPGA-based implementation and the general results of the study are evaluated in the conclusions part. systems.

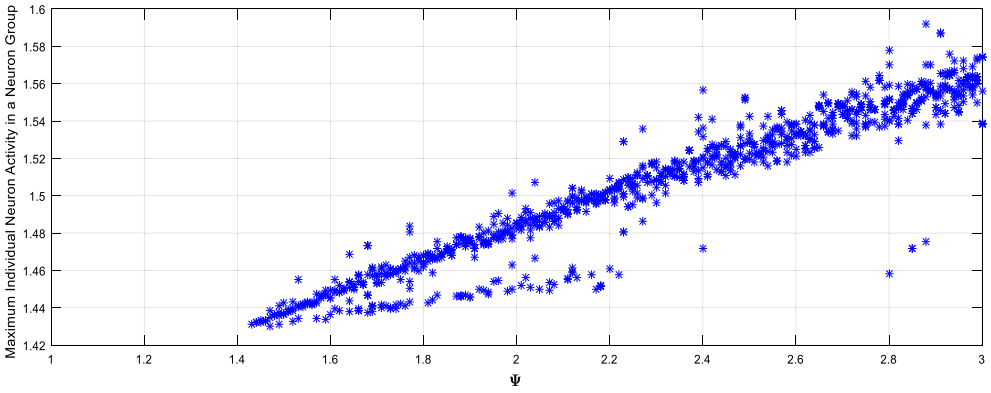

FIGURE 3. Bifurcation diagram results for observing the effect of the control parameter on the dynamical patterns of a neuron group.

II. ON SWIMMING PATTERN GENERATOR OF A LAMPREY

A lamprey is a primitive vertebrate animal. It has an alepidote skin and one or two dorsal fins. Their eyes are hidden under their skin. Their respiration and feeding are provided by water entering their mouth and extruding their gills. The body of a lamprey moves from head to tail with a lateral undulation and this movement is similar to a snake that moves through water [41]. The swimming pattern generator of a lamprey takes the considerations, because its anatomy and nervous system is simple, the oscillations on this patterns generator are able to measure and these primitive living beings are an inspiration for more complex vertebrates. Some basic assumptions have been made about the neurons and their interaction with each other in the swimming rhythmic pattern generator of a lamprey [9], [10], [11], [12], [13]. Some of these acceptances are as follows: i) There are reciprocally interacting neuron groups on the right and left sides in the swimming pattern generator of a lamprey, ii) These right and left neuron groups maintain to produce rhythmic patterns within themselves; even they are isolated from each other, iii) These neuron groups are coupled with each other through along the spinal cord of a lamprey (from head to tail), iv) One excitatory 'EIN', two inhibitory (one of them is laterally inhibitor neuron 'LIN' and another of them is collaterally inhibitor 'CIN' neurons) interneurons and one motor neuron 'M' are available in each neural group on the right and left sides, v) Each of these neurons interacts with each other, with the neurons on the opposite side, and with neighboring neural segments, vi) The neurons on the right and left sides fire in anti-phase, vii) There is a certain time delay between neuron firings in the each neural segment. The collaterally inhibitor neurons determine the neuronal behavior and they cause to start firing mechanisms. The neuronal activity is switched from one side to other side by the collaterally inhibitor neurons. While the neuronal activity increases thanks to the excitatory interneuron on one side, the collaterally inhibitor neurons cause to lessen neuronal activity on the other side. Thus, the neuronal activities on the opposite sides are induced in anti-phase [42].

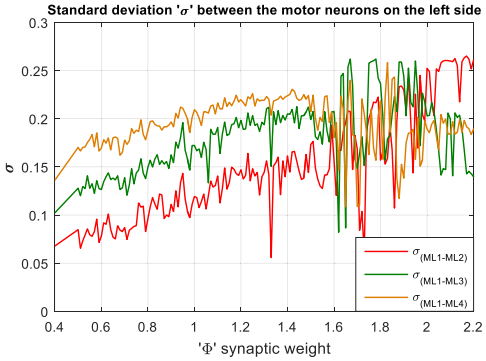

FIGURE 4. Standard deviation results between the motor neurons on the left sides.

The model, which has been presented to the literature by Anzinger & Rottoy [16], is expanded as in (1) in here for defining each neuron groups on the left or right side:

$$\begin{aligned}
\tau_{EIN_{side}}\frac{dEIN_{side}}{dt} &= -EIN_{side} + sign\,[2M_{side} - 1.4LIN_{side} \\
&\quad + M_{side_previous} - \Phi\, CIN_{opposite_side}] \\
\tau_{LIN_{side}}\frac{dLIN_{side}}{dt} &= -LIN_{side} + \Psi sign\,[EIN_{side} + M_{side}] \\
\tau_{M_{side}}\frac{dM_{side}}{dt} &= -M_{side} + sign\,[2EIN_{side} - 1.4LIN_{side}] \\
\tau_{CIN_{side}}\frac{dCIN_{side}}{dt} &= -CIN_{side} + sign\,[M_{side}]
\end{aligned} \tag{1}$$

In (1), the time constants are given the 'τ' parameters and they are adjusted to the following values: $\tau_{EIN_L} = 0.2$, $\tau_{LIN_L} = 3.5$, $\tau_{M_L} = 2.1$, $\tau_{CIN_L} = 0.2$, $\tau_{EIN_R} = 0.2$, $\tau_{LIN_R} = 6$, $\tau_{M_R} = 1$, $\tau_{CIN_R} = 0.2$.

Here, a representative illustration of a neuron group in (1) is given in Fig.2b and the outputs of the neurons are limited with a 'sign' function. This function set the output to one for the positive inputs or it set to the output minus one for the negative inputs, and the output is zero for zero input. In the referred study, this boundary function is a sigmoid-shape function and the limits of the sigmoid function lie between

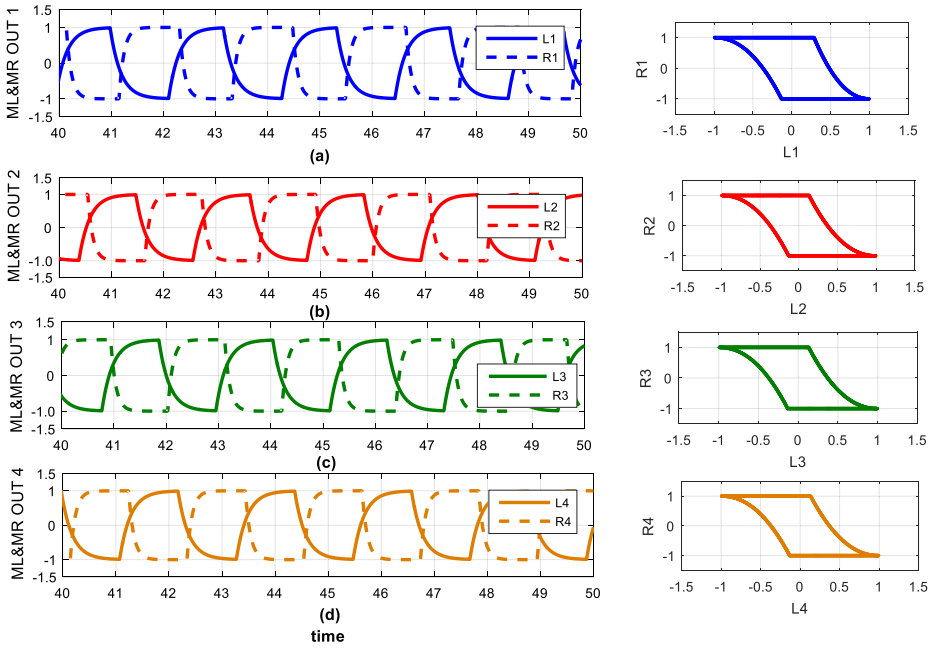

FIGURE 5. The numerical simulation results of the anti-phase firings between neuron groups on the right and left sides for four neural segments.

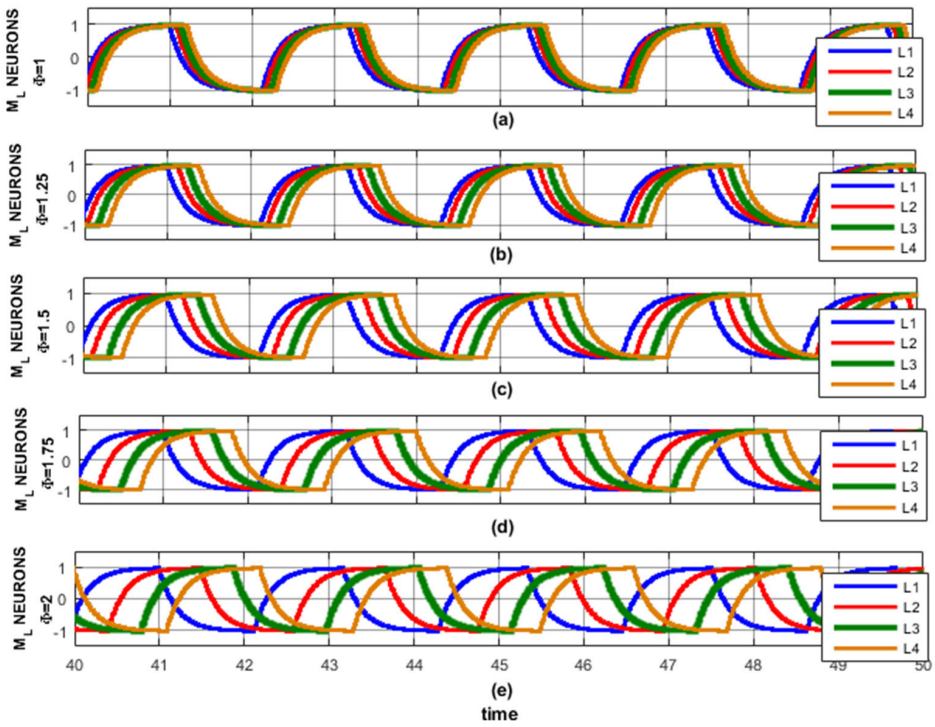

FIGURE 6. The numerical simulation results in time domain that show the effect of the 'reciprocal inhibition' connections on the time delays between neuron's firings for the a) $\Phi = 1$, b) $\Phi = 1.25$, c) $\Phi = 1.5$, d) $\Phi = 1.75$ and e) $\Phi = 2$ values.

zero and one. [16]. In fact, the direct revision is insufficient for getting individual rhythmic patterns in the neuron groups on the reciprocal sides. Thus, a control parameter 'Ψ' is included in the laterally interneuron of each neuron groups. The effect of this control parameter on the dynamical patterns of one neuron group is observed by the bifurcation diagram. The biological neuron models resemble oscillator structures. If the parameter values in the models are not selected correctly, they do not exhibit dynamiceal neuronal response. Bifurcation diagram is a graph and it is used to observe the change of the output dynamics over time versus to a control parameter change in the system, simultaneously. The

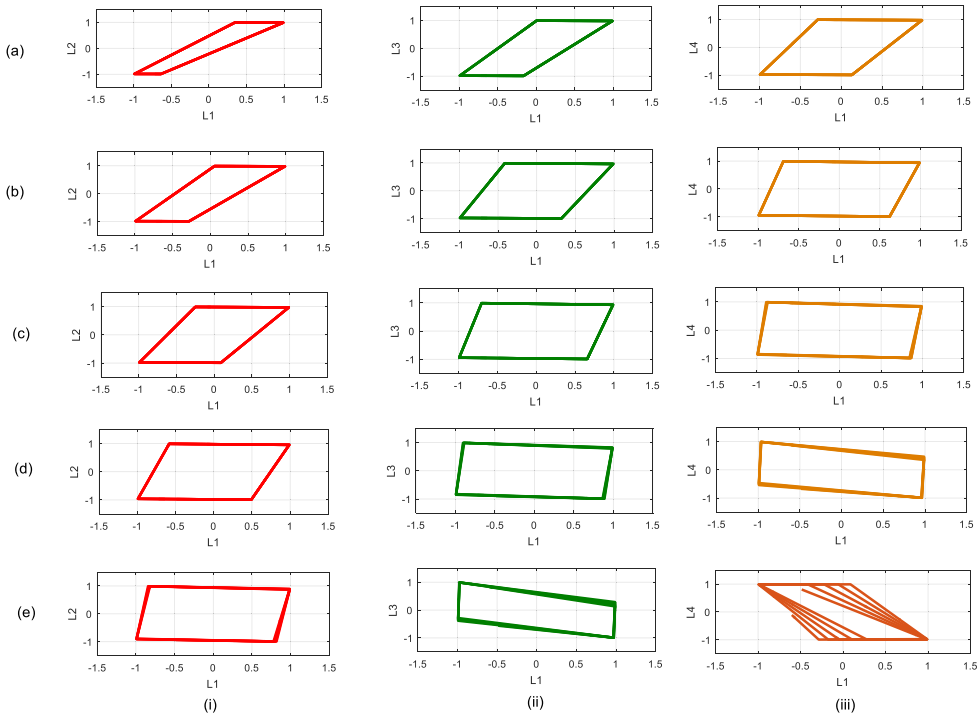

FIGURE 7. The comparison between the phase portraits of the left motor neurons in Fig.1 for observing the time delays between the neural segments: The phase differences between i) the ML1-ML2 neurons, ii) the ML1-ML3 neurons and iii) the ML1-ML4 neurons for the a) $\Phi = 1$, b) $\Phi = 1.25$, c) $\Phi = 1.5$, d) $\Phi = 1.75$ and e) $\Phi = 2$ values.

horizontal axis represents the change of the control parameter and the vertical axis represents the output dynamics of the system. In here, parameter research is executed from one to three with the '0.01' step size and the time-span is adjusted to '0-300ms'. Its result is seen in Fig.3. According to the result in Fig.3, since no neural output dynamics can be observed in the$1 < \Psi < 1.4$ range, approximately, it can be concluded that the individual neurons in a neuron group do not produce a dynamical pattern. As the value of the control parameter increases, the activities of the neurons also increase. Since high amplitude-neurons are not desired, the value of the control parameter is set to '1.6' in the all-neuron groups of the swimming pattern generator network in Fig.2a.

After that, we focus on the effect of 'Φ' parameter in (1) on this swimming pattern generator. When the studies about central pattern generator structures in the literature are examined, it is stated that 'reciprocal inhibition' is also effective as a source of time delays between neuron firings [8], [32]. The asymmetric body movements are produced by the central nervous systems of the living being and it is thought that the 'reciprocal inhibition' is the source of the asymmetrical activations on the left and right sides, biologically [43]. In addition, the inhibition and excitation states that exist in the chemical synapse structures between neurons are related to the properties of the neurotransmitter substance. These states, which are the source of information transfer between neurons, is associated with the concept of synaptic weight in the mathematical modeling process. The value of the synaptic weight parameter is directly related to the concept of the synchronization between neurons. At the optimum value of synaptic weight, the dynamical firings of two neurons are simultaneous. On the other hand, as the synaptic weight value changes, a time delay occurs between firing times of the coupled neurons. Thus, the 'Φ' parameter is included in the model as a synaptic weight parameter. This parameter represents a synaptic connection from the collaterally inhibitor neuron on one side to the excitatory neurons on the opposite side and it is represented by the variable resistors in Fig.2b. This parameter has a changeable characteristic in all neural segments except from the first neural segment, namely it is equal to one in the first neural segments. Here, it is aimed to get a certain time delay between neural segments of the swimming pattern generator network. Even better, it is also observed that the amount of this delay can be adjusted by changing the values of this synaptic weight parameter. Additionally, all exhibitory interneurons take an input from the motor neurons in the previous neural segment as seen in Fig.2a, but the exhibitory interneurons in the first neuronal segments take a stimulus signal instead of the motor neuron signal in the previous neural segment. The value of this stimulation is equal to the '0.6' on the both sides. Standard deviation results between the coupled neurons offer an idea about their synchronized or unsynchronized firings [27], [44]. As their dynamical behaviors get close to each other, standard deviation result converges to zero, otherwise, it shows an increasing trend. In this study, the standard deviation results

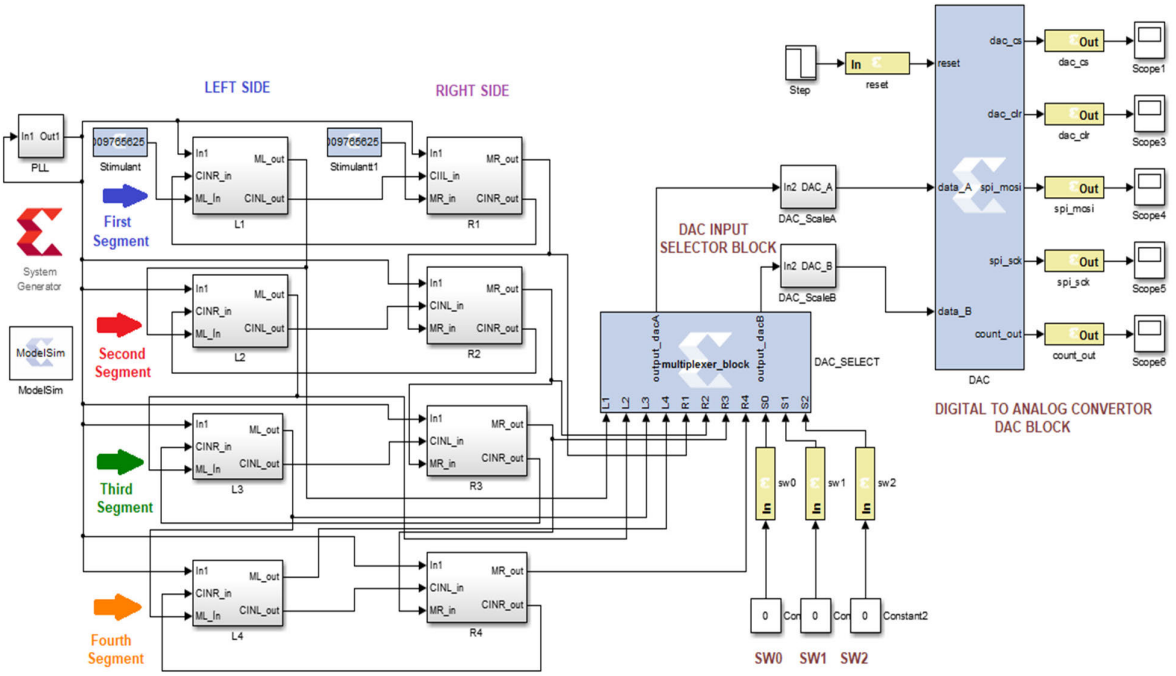

(a)

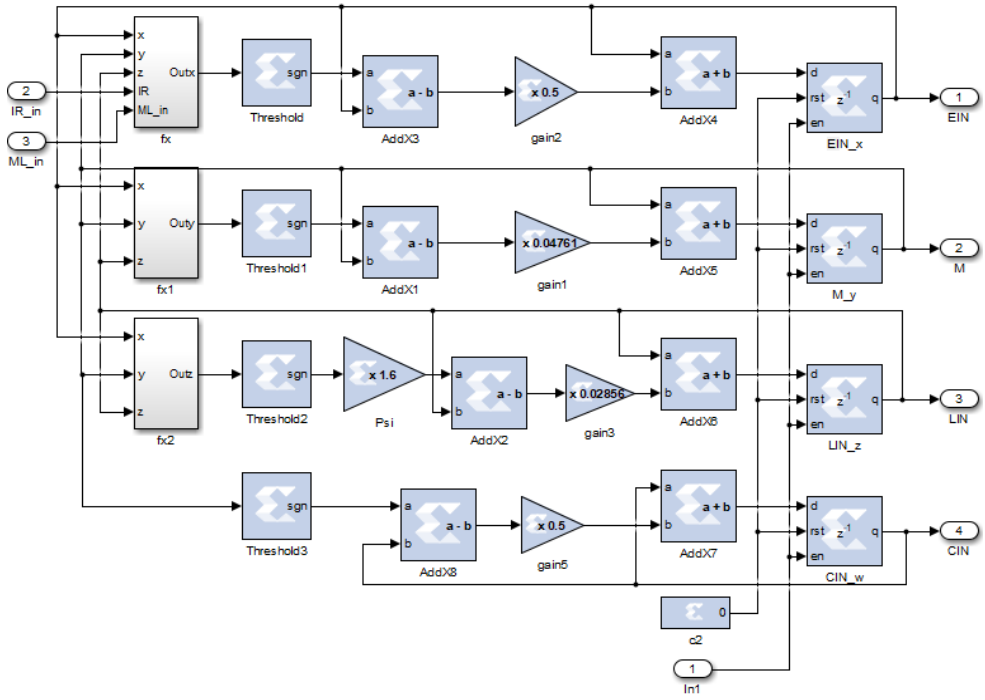

(b)

FIGURE 8. a) The constructed blocks for implementing the swimming pattern generator network in Fig.2a, b) The constructed block for implementing a neuron group in any side in Fig.2b on the FPGA.

of the motor neurons on the left sides are given in Fig.4 depending on the effect of 'Φ' parameter. The red line is the standard deviation between ML1 and ML2 neurons. The green line belongs to the ML1 and ML3 neurons. The orange line represents the standard deviation between ML1 and ML4 neurons. The red line is closer to zero and the standard deviation represented by orange line is the highest one. According to these graphs, while the closest characteristic to the dynamical behavior of the ML1 neuron belongs to ML2, the furthest characteristic belongs to ML4. Moreover, as the value of the

control parameter increases, the standard deviation results also increase, and the dynamical behavior of all neurons moves away from the ML1 neuron. Accordingly, the effect of the 'Φ' parameter on the time delay between neurons is seen clearly. The parameter is changed in range 0.4 and 2.2, and it is observed that as its value increases, the standard deviation results also increases.

In here, the numerical simulation results of the anti-phase firings between neuron groups on the right and left sides for four neural segments are given in Fig.5. The numerical simulation results that show the effect of the 'reciprocal inhibition' connections on the time delays between neuron firings are presented in Fig.6. This figure includes five different time-delayed results for the $'\Phi = 1, \Phi = 1.25, \Phi = 1.5, \Phi = 1.75, \Phi = 2$' values. From these numerical simulation results, it is seen that the increasing of the 'Φ' synaptic weight parameter causes the increased time delays between the neural segments. The phase attractors, which are plotted by using X-Y plot feature of the measurement systems, allow observing the phase differences between the input signals such as Lissajous pattern [45]. Thus, the phase domain illustrations of the left motor neuron in the first segment and the other left motor neurons in the next segments are plotted for the values given above ($'\Phi = 1, \Phi = 1.25, \Phi = 1.5, \Phi = 1.75, \Phi = 2$), respectively. The results of these numerical simulations are given in Fig.7. According to Fig.7, the phase differences between ML1-ML2 neurons increase as the synaptic weight values increase (from Fig.7i.a to 7i.e). Similarly, while the phase differences between ML1-ML3 neurons are given from Fig. 7ii.a to Fig.7ii.e, ones of ML1-ML4 are seen in from Fig. 7iii.a to Fig. 7iii.e. Their phase differences are also increases with the increment of the synaptic weights. Additionally, the phase differences between the ML1-ML4 neurons' are bigger than the ML1-ML3's and the ones of the ML1-ML3 neurons are bigger than the ML1-ML2 neurons'. According to these results, the change of the 'Φ' parameters, which represents the synaptic connection from the collaterally inhibitor interneuron to the excitatory interneuron on the opposite side, causes an equivalent time delay in consecutive neural segments of the swimming pattern generator network. These numerical simulations are performed on the MATLAB-SIMULINK^{TM} numerical simulation tool by using the Dormand-Prince integration algorithm.

III. OBTAINING THE ELECTRICAL SIGNALS WITH FPGA FOR A NEUROMORPHIC SWIMMING PATTERN GENERATOR

A neuromorphic system describes the designing of an electronic circuitry that is emulate any capability of a living being, so various bio-inspired developments, which are transferred the biological mains to the engineering applications, are presented to the literature [22], [23], [24]. The pattern generator networks are one of the most critical application fields of the neuromorphic studies. After the modeling of these rhythmic patterns, these models are able to be realized by various electronic equipment.

TABLE 1. The states of the switches and the outputs of the multiplexer block.

SW2	SW1	SW0	DAC A	DAC B
0	0	0	ML1	MR1
0	0	1	ML2	MR2
0	1	0	ML3	MR3
0	1	1	ML4	ML4
1	0	0	ML1	ML2
1	0	1	ML1	ML3
1	1	0	ML1	ML4
1	1	1	ML1	ML1

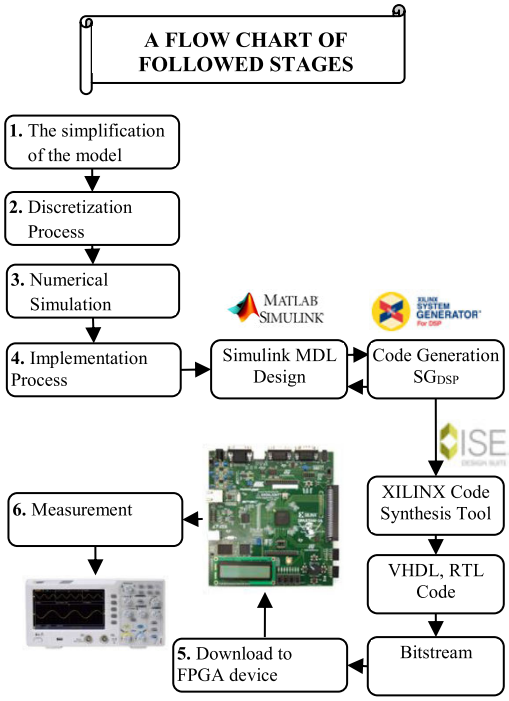

FIGURE 9. A flow chart for the design procedure of the swimming pattern generator implementation with FPGA.

There are many examples in the literature regarding the usage of the analog or digital equipment in the realization of these structures [33], [34], [35], [36]. However, the FPGA device is one of the most preferred hardware in the implementations of the rhythmic pattern generators [37], [38], [39], [40]. FPGAs are among the pioneer electronic equipment to verify prototype designs; thanks to its programmability feature and parallel working principle. In this study, the SPARTAN-3AN FPGA board of XILINX^{TM} company is used and it is utilized from the 'System Generator for DSP tool' for constructing the swimming pattern generator network in Fig.2a on this FPGA board [46].

In this process, this swimming network is designed as in Fig.8a on the 'System Generator for DSP tool' of the MATLAB-SIMULINK^{TM}. There are several tools to synthesize the hardware description language codes from a high-level description to a gate-level synthesis on FPGA. The 'System Generator for DSP tool' generates the bitstreams to program the FPGA device and the RTL synthesis in the

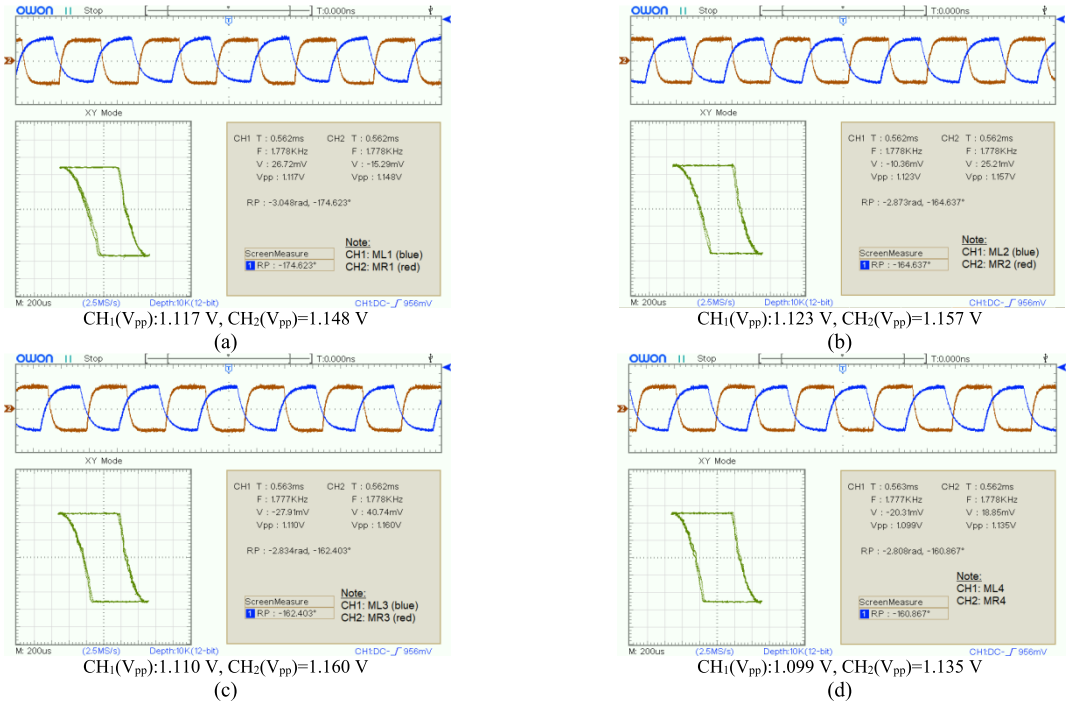

FIGURE 10. The measured electrical signals from the FPGA device for the anti-phase firings in the a) first neural segment (ML1 & MR1), b) second neural segment (ML2 & MR2), c) third neural segment (ML3 & MR3) and d) fourth neural segment (ML4 & MR4) of the swimming pattern generator.

gate level design are routed in FPGA automatically with this tool. In Fig.8a, there are four neural segments similar to Fig.2a and each of these neural segments contains two neuron groups, left and right. All of these neuron groups include one excitatory interneuron, one laterally inhibitory interneuron, one collaterally inhibitory interneuron and one motor neuron and a total of thirty-two neurons are constructed on FPGA. The constructed block for implementing a neuron group in any side in Fig.2b on the FPGA are seen in Fig.8b. As seen from Fig.8b, the neuron definitions in (1) transform to a discretize system by the Euler Method and the constant that defines the step size is taken as '0.1'. The integrator definition in (1) is converged by using Euler method and the next values of the calculations are hold by a register block for each state variable. The multiplications with constants are obtained with the gain, right and left register blocks. The 'sign' function is constructed by using the conditional decision expressions. The remaining operations are combined with the mathematical operands. In Fig.8a, the 'Phase-Locked Loop-PLL' block adjusts the clock frequency and this block triggers the registers in the sequential circuit. The 'Digital to Analog Convertor-DAC' is LTC2624. This DAC is a dual 12-bit, it works with I^2C protocol and it has two channels (A and B). The outputs are measured through this DACs. The 'multiplexer block' in Fig.8a selects the input signals of the DAC blocks. In the multiplexer block, three switches are used for selecting two of eight different input signals and these selected inputs are sent to the A and B channels of the DAC block. Two input channels of the DAC block are defined according to the states of switches as in Table 1:

According to this table, the analog electrical signals at the output of the DAC are able to observe consistent with the results in Figs.5, 6 and 7. The anti-phase firings (from the ML1-MR1 to ML4- MR4 neurons) in each neural segments are measured by adjusted the switches from SW2=0, SW1=0, SW0=0 to SW2=0, SW1=1, SW0=1, respectively. After changing the synaptic weight parameters, the time-delayed firings of the neurons in each neural segment are also measured by controlling the states of these switches (from SW2=1, SW1=0, SW0=0 to SW2=1, SW1=1, SW0=0). 'Very high-speed integrated circuit Hardware Description Language-VHDL' codes are obtained by a code transformation process between the System Generator for DSP and the XILINX^{TM} core. After this transformation, the bitstream of RTL level design is downloaded to SPARTAN-3AN FPGA devices. These codes are embedded to FPGA devices and the measurements are recorded by a digital oscilloscope. A flow chart for the design procedure of the swimming pattern generator implementation with FPGA is summarized in Fig.9.

The measured electrical signals from the FPGA device through the DAC are presented in Fig. 10 for the anti-phase firings in each segment. The 'Φ' synaptic weight parameters are fixed to one in these measurements. The experimental implementation results that show the effect of the 'reciprocal inhibition' connections on the time delays between neuron firings are presented in Fig. 11. This figure includes five

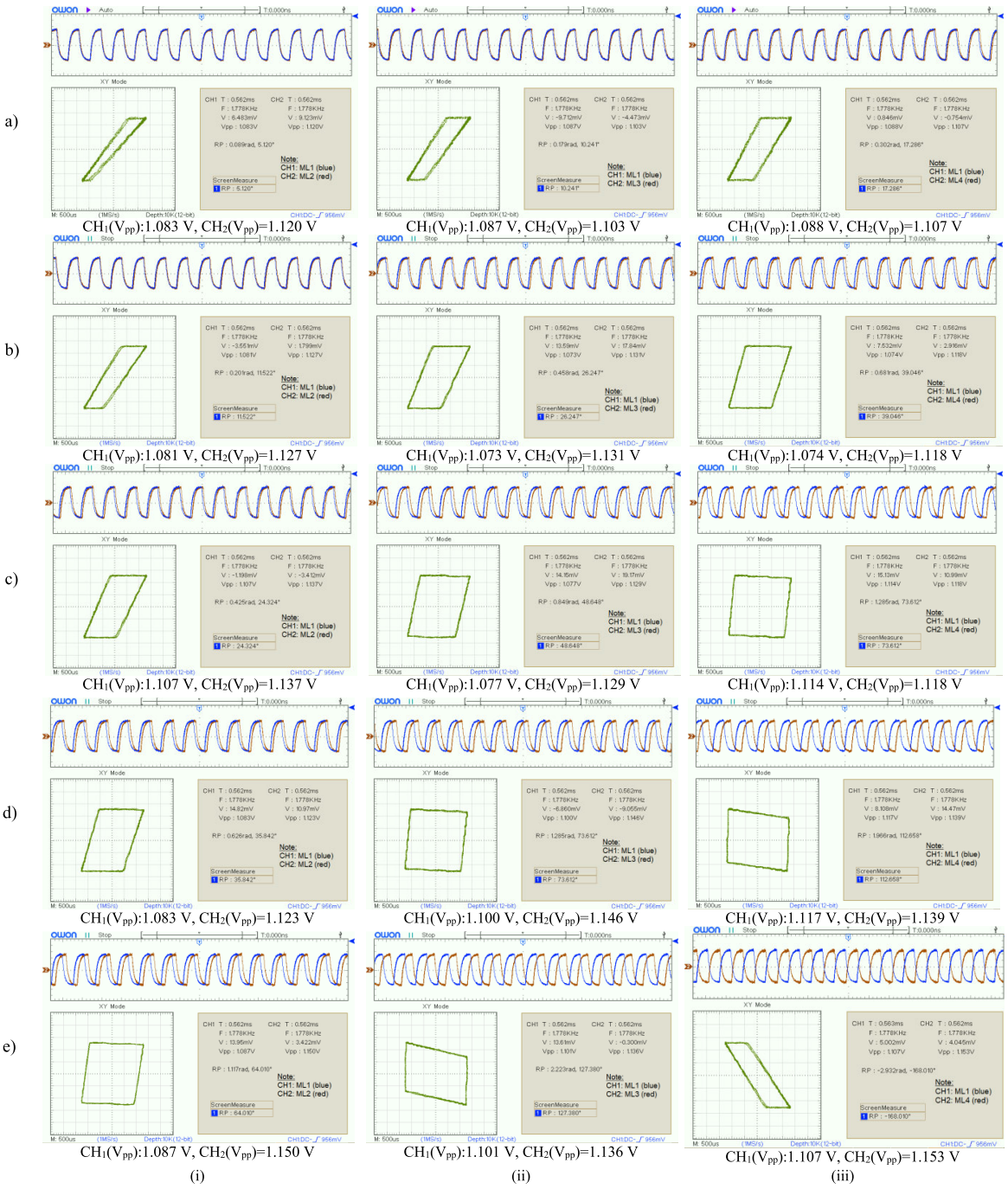

FIGURE 11. The measured electrical signals with the FPGA device for showing the effect of the 'reciprocal inhibition' connections on the time delays between neuron's firings: Time domain and phase portrait illustrations of i) the ML1-ML2 neurons, ii) the ML1-ML3 neurons and iii) the ML1-ML4 neurons for the a) $\Phi = 1$, b) $\Phi = 1.25$, c) $\Phi = 1.5$, d) $\Phi = 1.75$ and e) $\Phi = 2$ values.

different time-delayed results. The amounts of these delays are recorded by measuring the phase differences between the left motor neurons in the neural segments. In the numerical simulation results, the time domain responses and the phase attractors of the left motor neurons have been observed by two different illustrations (Fig.6 and Fig.7), separately. On the other hand, these results are presented together in the realization stage by utilizing an illustration feature of the used oscilloscope. The DAC outputs on FPGA are connected to the oscilloscope channels. The phase differences between neural segments are measured by utilizing the phase measurement option of a digital oscilloscope and the electrical signals obtained by the FPGA device are recorded by this oscilloscope. An experimental setup illustration is given in Fig.12. During the realization stages, the 'Φ' synaptic weight parameters are also adjusted to the '$\Phi = 1, \Phi = 1.25, \Phi = 1.5, \Phi = 1.75, \Phi = 2$' values, separately and the recorded results for the values are given from Fig.11a to 11e,

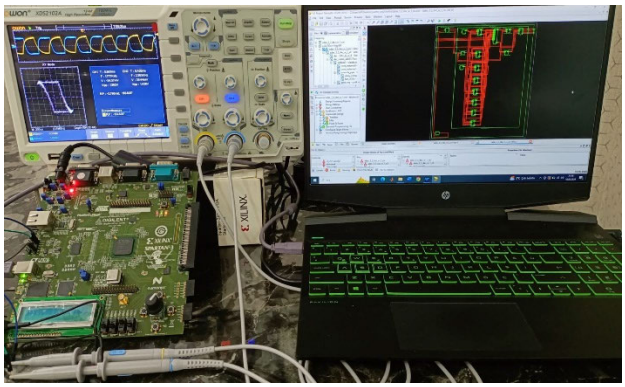

FIGURE 12. An experimental setup illustration for measuring the electrical signals obtained by the FPGA device via an oscilloscope.

TABLE 2. The measured phase differences between the neural segments for observing the effect of the synaptic weight parameters on the time delays block.

The 'Φ' synaptic weight parameters	The measured phase differences		
	ML1-ML2	ML1-ML3	ML1-ML4
a) Φ=1	5.120^0	10.241^0	17.286^0
b) Φ=1.25	11.522^0	26.247^0	39.046^0
c) Φ=1.5	24.328^0	48.648^0	73.612^0
d) Φ=1.75	35.842^0	73.612^0	112.658^0
e) Φ=2	64.010^0	127.280^0	$-168.010^0(191.990^0)$

respectively. According to the results given in Fig.11, the measured phase differences between the neural segments are summarized in the Table 2 for observing the effect of the synaptic weight parameters on the time delays. As seen from Table 2, when the 'Φ' synaptic weight parameters are set a value, the phase differences of the consecutive neural segments increase by approximately equal steps.

For example, the 'Φ' synaptic weight parameters are equal to '1.5', the phase differences of the ML1-ML2, ML1-ML3 and ML1-ML4 neurons are measured as 24.328^0, 48.648^0 and 73.612^0. The phase difference between the consecutive segments has been recorded as approximately 24^0 degrees for 'Φ = 1.5'. On the other hand, the increasing of the 'Φ'synaptic weight parameters also increases the phase difference between the neuron groups. For example, while the phase differences between ML1-ML3 neuron groups is equal to 10.241^0 for 'Φ = 1', this difference has been measured as 48.648^0 and 127.280^0 for 'Φ = 1.5' and 'Φ = 2', respectively. Therefore, the time delay effect of the synaptic weight parameters, which are included in the system as a 'reciprocal inhibition', has been also confirmed by the hardware implementations. These obtained phase correlations between the motor neurons are the result of the synaptic weight parameter changes.

IV. CONCLUSION

This study focuses on the swimming pattern generator of a lamprey that is a well-known neural circuit. A previously proposed model, which is described the interactions of the swimming pattern generator's neurons, has been extended for adapting to a digital implementation. While a sigmoid-shaped transfer function has been used for limiting the activities of the neurons in the previous version of this model, the usage of a 'sign' function is offered instead of this sigmoid-shape function for digital implementation easiness in here. However, additionally, a control parameter has been added to the laterally interneurons in the swimming pattern generator model because of the insufficiency of the 'sign' function's direct usage. The result of the bifurcation diagram has been used for observing the response of the system to the change of this control parameter. The value of this control parameter has been determined as '1.6'. Then, a four-segmented neural swimming pattern generator has been designed and the numerical simulation stage has been performed via this network. Since the lampreys resemble swimming snakes, they move by utilizing asymmetric fired-patterns that are produced in swimming pattern generators. While these movements are occurring, it is very important that the neuron groups on the right and left sides of the lamprey's swimming pattern generator fire in opposite phases. Thus, one of the characteristic assumptions about the lamprey's swimming pattern generator is that the neuron groups on the opposite sides fire in anti-phase. The numerical simulation results of these anti-phase firing have been observed for each segment in this designed network and their results has been given in Fig.5.

In addition, the 'reciprocal inhibition' synaptic connections have been adapted to the swimming pattern generator model. The collaterally inhibitor interneurons in one side are connected to the exhibitory inter neurons in the opposite side with a variable synaptic weight parameter. The time delay between the firings of the coupled neurons changes depending on the values of the synaptic weight. The synchrony or asynchrony firings between the coupled neuron can be observed by utilizing standard deviation results, so several standard deviation results have been given for getting a foresight about the time delays between the neurons. Since these delays can be measured by observing the phase attractors, the additional numerical simulations have been also performed for five different synaptic weight values in order to observe the effect of these parameters on the time delay between the neural segments. The results of these numerical simulations are presented in Figs.6 and 7, and they confirm the conclusion that the synaptic weight parameter provides an adjustable time delay.

The final aim of this study has been offered as designing a neuromorphic digital circuit that is able to emulate the swimming rhythmic patterns of a lamprey. For this reason, a digital realization has been carried out by using the 'sign' function-based revised pattern generator model. In this implementation process, the digital programmable FPGA device has been used and the obtained electrical signals have been given in Figs.10 and 11. The used element quantities on the FPGA device are summarized in Table 3.

TABLE 3. The used element quantities on the FPGA device.

LOGIC UTILIZATION	USED	AVAILABLE	UTILIZATION
Total Number Slice Registers	1066	11776	9%
Number of 4 input LUTs	8526	11776	72%
Number of occupied Slices	5131	5888	87%
Total Number of 4 input LUTs	9922	11776	84%
Number of bonded IOBs	18	372	4%
Number of BUFGMUXs	2	24	8%
Number of MULT18X18SIOs	0	20	0%
Max.Time delay (ns)	1.124	-	-

TABLE 4. The details of the power consumption in the FPGA device.

ON-CHIP	POWER(W)	USED	AVAILABLE
Clocks	0.010	2	-
Logic	0.000	9922	11776
Signals	0.000	12606	-
IOs	0.000	18	372
Leakage	0.036	-	-
Total	0.047	-	-

One of the most encountered problems in the digital device-based implementations of the nonlinear systems is the limited number of multiplier blocks. For example, the SPARTAN-3AN FPGA board of XILINX^{TM} company has twenty multiplier blocks. Thus, the realization studies performed using as few as possible multiplier block take the attentions in the literature [47], [48], [49], [50], [51]. From Table 3, it is seen that no multiplier block has been used in the FPGA-based implementation of this swimming pattern generator thanks to the simplification process of the transfer function. This outcome makes more valuable the provided contribution in here. The power consumption in this programmable digital element is also very low. Details about the consumed power in this FPGA device are summarized in Table 4:

Moreover, the anti-phase firings of the neuron groups on the opposite sides and getting an adjustable time delay between neural segments have been also achieved in the hardware implementation process, successfully. The electrical signals have been gotten by these realizations and these electrical signals may also enable to carry out several experiments without interfering with the living being. Since these obtained electrical signals can be used in the control of the actuators of the swimming robots, they are also suitable for using in the electromechanical systems.

REFERENCES

[1] F. Delcomyn, "Neural basis of rhythmic behavior in animals," *Science*, vol. 210, no. 4469, pp. 492–498, Oct. 1980, doi: 10.1126/science.7423199.
[2] P. S. G. Stein, S. Grillner, A. Selverston, and D. G. Stuart, *Neurons, Networks, and Motor Behavior*. Cambridge, MA, USA: MIT Press, 1999, p. 307.
[3] E. Marder and R. L. Calabrese, "Principles of rhythmic motor pattern generation," *Physiolog. Rev.*, vol. 76, no. 3, pp. 687–717, Jul. 1996.
[4] S. Rossignol, R. Dubuc, and J.-P. Gossard, "Dynamic sensorimotor interactions in locomotion," *Physiolog. Rev.*, vol. 86, no. 1, pp. 89–154, Jan. 2006, doi: 10.1152/physrev.00028.2005.
[5] S. Grillner, A. P. Georgopoulos, and L. M. Jordan, "Selection and initiation of motor behavior," in *Neurons, Networks, and Motor Behavior*, P. S. G. Stein, S. Grillner, A. Selverston, and D. G. Stuart, Eds. London, U.K.: MIT Press, 1999.
[6] S. Grillner, "Neural control of vertebrate locomotion—Central mechanisms and reflex interaction with special reference to the cat," in *Feedback and Motor Control in Invertebrates and Vertebrates*, W. J. P. Barnes and C. Helm, Eds. Dordrecht, The Netherlands: Springer, 1985, doi: 10.1007/978-94-011-7084-0_3.
[7] P. A. Guertin, "The mammalian central pattern generator for locomotion," *Brain Res. Rev.*, vol. 62, no. 1, pp. 45–56, Dec. 2009, doi: 10.1016/j.brainresrev.2009.08.002.
[8] A. I. Selverston, "Invertebrate central pattern generator circuits," *Phil. Trans. Roy. Soc. B, Biol. Sci.*, vol. 365, no. 1551, pp. 2329–2345, Aug. 2010, doi: 10.1098/rstb.2009.0270.
[9] S. Grillner and P. Wallén, "How does the lamprey central nervous system make the lamprey swim?" *J. Experim. Biol.*, vol. 112, no. 1, pp. 337–357, Sep. 1984.
[10] S. Grillner, P. Wallén, N. Dale, L. Brodin, J. Buchanan, and R. Hill, "Transmitters, membrane properties and network circuitry in the control of locomotion in lamprey," *Trends Neurosciences*, vol. 10, no. 1, pp. 34–41, Jan. 1987, doi: 10.1016/0166-2236(87)90123-8.
[11] J. T. Buchanan, "Neural network simulations of coupled locomotor oscillators in the lamprey spinal cord," *Biol. Cybern.*, vol. 66, no. 4, pp. 367–374, Feb. 1992, doi: 10.1007/bf00203673.
[12] J. T. Buchanan, "Contributions of identifiable neurons and neuron classes to lamprey vertebrate neurobiology," *Prog. Neurobiol.*, vol. 63, no. 4, pp. 441–466, Mar. 2001, doi: 10.1016/s0301-0082(00)00050-2.
[13] A. J. Ijspeert, A. Crespi, D. Ryczko, and J.-M. Cabelguen, "From swimming to walking with a salamander robot driven by a spinal cord model," *Science*, vol. 315, no. 5817, pp. 1416–1420, Mar. 2007, doi: 10.1126/science.1138353.
[14] Ö. Ekeberg, P. Wallén, A. Lansner, H. Travén, L. Brodin, and S. Grillner, "A computer based model for realistic simulations of neural networks: I. The single neuron and synaptic interaction," *Biol. Cybern.*, vol. 65, no. 2, pp. 81–90, Jun. 1991, doi: 10.1007/bf00202382.
[15] Ö. Ekeberg, "A combined neuronal and mechanical model of fish swimming," *Biol. Cybern.*, vol. 69, nos. 5–6, pp. 363–374, Oct. 1993, doi: 10.1007/bf00199436.
[16] M. Anzinger and F. Rattay, "The role of inhibition in central pattern generators: A simulation study," *Neurocomputing*, vol. 72, nos. 7–9, pp. 2032–2034, Mar. 2009, doi: 10.1016/j.neucom.2008.11.012.
[17] R. Jung, E. J. Brauer, and J. J. Abbas, "Real-time interaction between a neuromorphic electronic circuit and the spinal cord," *IEEE Trans. Neural Syst. Rehabil. Eng.*, vol. 9, no. 3, pp. 319–326, Sep. 2001, doi: 10.1109/7333.948461.
[18] I. Youssef, M. Mutlu, B. Bayat, A. Crespi, S. Hauser, J. Conradt, A. Bernardino, and A. Ijspeert, "A neuro-inspired computational model for a visually guided robotic lamprey using frame and event based cameras," *IEEE Robot. Autom. Lett.*, vol. 5, no. 2, pp. 2395–2402, Apr. 2020, doi: 10.1109/LRA.2020.2972839.
[19] P. Dario, C. Stefanini, A. Menciassi, C. Laschi, and F. Vecchi, "Towards a new generation of hybrid bionic systems for telepresence: The lamprey model," in *Proc. 15th IEEE Int. Symp. Robot Human Interact. Commun.*, Sep. 2006, pp. 497–501, doi: 10.1109/ROMAN.2006.314377.
[20] A. J. Ijspeert and A. Crespi, "Online trajectory generation in an amphibious snake robot using a lamprey-like central pattern generator model," in *Proc. IEEE Int. Conf. Robot. Autom.*, Rome, Italy, Apr. 2007, pp. 262–268, doi: 10.1109/ROBOT.2007.363797.
[21] Z. Huang, S. Ma, H. Bagheri, C. Ren, and H. Marvi, "The impact of dorsal fin design on the swimming performance of a snake-like robot," *IEEE Robot. Autom. Lett.*, vol. 7, no. 2, pp. 4939–4944, Apr. 2022, doi: 10.1109/LRA.2022.3153903.
[22] Y. A. Tsybina, S. Y. Gordleeva, A. I. Zharinov, I. A. Kastalskiy, A. V. Ermolaeva, A. E. Hramov, and V. B. Kazantsev, "Toward biomorphic robotics: A review on swimming central pattern generators," *Chaos, Solitons Fractals*, vol. 165, Dec. 2022, Art. no. 112864, doi: 10.1016/j.chaos.2022.112864.

[23] R. George, M. Chiappalone, M. Giugliano, T. Levi, S. Vassanelli, J. Partzsch, and C. Mayr, "Plasticity and adaptation in neuromorphic biohybrid systems," *iScience*, vol. 23, no. 10, Oct. 2020, Art. no. 101589, doi: 10.1016/j.isci.2020.101589.
[24] P. Lopez-Osorio, A. Patiño-Saucedo, J. P. Dominguez-Morales, H. Rostro-Gonzalez, and F. Perez-Peña, "Neuromorphic adaptive spiking CPG towards bio-inspired locomotion," *Neurocomputing*, vol. 502, pp. 57–70, Sep. 2022, doi: 10.1016/j.neucom.2022.06.085.
[25] H. Soleimani, A. Ahmadi, and M. Bavandpour, "Biologically inspired spiking neurons: Piecewise linear models and digital implementation," *IEEE Trans. Circuits Syst. I, Reg. Papers*, vol. 59, no. 12, pp. 2991–3004, Dec. 2012, doi: 10.1109/TCSI.2012.2206463.
[26] N. Korkmaz, İ. Öztürk, A. Kalinli, and R. Kiliç, "A comparative study on determining nonlinear function parameters of the Izhikevich neuron model," *J. Circuits, Syst. Comput.*, vol. 27, no. 10, Sep. 2018, Art. no. 1850164, doi: 10.1142/S0218126618501645.
[27] N. Korkmaz, İ. Öztürk, and R. Kılıç, "The investigation of chemical coupling in a HR neuron model with reconfigurable implementations," *Nonlinear Dyn.*, vol. 86, no. 3, pp. 1841–1854, Nov. 2016, doi: 10.1007/s11071-016-2996-6.
[28] S. Haghiri and A. Ahmadi, "A novel digital realization of AdEx neuron model," *IEEE Trans. Circuits Syst. II, Exp. Briefs*, vol. 67, no. 8, pp. 1444–1448, Aug. 2020, doi: 10.1109/TCSII.2019.2938180.
[29] E. Jokar, H. Abolfathi, A. Ahmadi, and M. Ahmadi, "An efficient uniform-segmented neuron model for large-scale neuromorphic circuit design: Simulation and FPGA synthesis results," *IEEE Trans. Circuits Syst. I, Reg. Papers*, vol. 66, no. 6, pp. 2336–2349, Jun. 2019, doi: 10.1109/TCSI.2018.2889974.
[30] J. Zhao and Y.-B. Kim, "Circuit implementation of FitzHugh–Nagumo neuron model using field programmable analog arrays," in *Proc. 50th Midwest Symp. Circuits Syst.*, Montreal, QC, Canada, Aug. 2007, pp. 772–775, doi: 10.1109/MWSCAS.2007.4488691.
[31] N. Korkmaz and R. Kilic, "Implementations of modified chaotic neural models with analog reconfigurable hardware," *Int. J. Bifurcation Chaos*, vol. 24, no. 4, Apr. 2014, Art. no. 1450046, doi: 10.1142/s0218127414500461.
[32] S. Grillner, "Biological pattern generation: The cellular and computational logic of networks in motion," *Neuron*, vol. 52, no. 5, pp. 751–766, Dec. 2006, doi: 10.1016/j.neuron.2006.11.008.
[33] M. A. Lewis, M. J. Hartmann, R. Etienne-Cummings, and A. H. Cohen, "Control of a robot leg with an adaptive aVLSI CPG chip," *Neurocomputing*, vols. 38–40, pp. 1409–1421, Jun. 2001, doi: 10.1016/s0925-2312(01)00506-9.
[34] Z. Yang, K. Cameron, W. Lewinger, B. Webb, and A. Murray, "Neuromorphic control of stepping pattern generation: A dynamic model with analog circuit implementation," *IEEE Trans. Neural Netw. Learn. Syst.*, vol. 23, no. 3, pp. 373–384, Mar. 2012, doi: 10.1109/TNNLS.2011.2177859.
[35] L. Li, C. Wang, and G. Xie, "A general CPG network and its implementation on the microcontroller," *Neurocomputing*, vol. 167, pp. 299–305, Nov. 2015, doi: 10.1016/j.neucom.2015.04.066.
[36] E. Donati, F. Corradi, C. Stefanini, and G. Indiveri, "A spiking implementation of the lamprey's central pattern generator in neuromorphic VLSI," in *Proc. IEEE Biomed. Circuits Syst. Conf. (BioCAS)*, Lausanne, Switzerland, Oct. 2014, pp. 512–515.
[37] M. Ambroise, T. Levi, S. Joucla, B. Yvert, and S. Saïghi, "Real-time biomimetic central pattern generators in an FPGA for hybrid experiments," *Frontiers Neurosci.*, vol. 7, no. 215, pp. 1–11, 2013, doi: 10.3389/fnins.2013.00215.
[38] N. Korkmaz, İ. Öztürk, and R. Kiliç, "Modeling, simulation, and implementation issues of CPGs for neuromorphic engineering applications," *Comput. Appl. Eng. Educ.*, vol. 26, no. 4, pp. 782–803, Jul. 2018, doi: 10.1002/cae.21972.
[39] Q. Chen, J. Wang, S. Yang, Y. Qin, B. Deng, and X. Wei, "A real-time FPGA implementation of a biologically inspired central pattern generator network," *Neurocomputing*, vol. 244, pp. 63–80, Jun. 2017, doi: 10.1016/j.neucom.2017.03.028.
[40] J. H. Barron-Zambrano and C. Torres-Huitzil, "FPGA implementation of a configurable neuromorphic CPG-based locomotion controller," *Neural Netw.*, vol. 45, pp. 50–61, Sep. 2013, doi: 10.1016/j.neunet.2013.04.005.
[41] V. V. Lamprey. (2014). *The Canadian Encyclopedia*. Accessed: Nov. 10, 2023. [Online]. Available: https://www.thecanadianencyclopedia.ca/en/article/lamprey
[42] A. J. Ijspeert and J. Kodjabachian, "Evolution and development of a central pattern generator for the swimming of a lamprey," *Artif. Life*, vol. 5, no. 3, pp. 247–269, Jul. 1999, doi: 10.1162/106454699568773.
[43] T. Shimazaki, M. Tanimoto, Y. Oda, and S.-I. Higashijima, "Behavioral role of the reciprocal inhibition between a pair of mauthner cells during fast escapes in zebrafish," *J. Neurosci.*, vol. 39, no. 7, pp. 1182–1194, Feb. 2019, doi: 10.1523/jneurosci.1964-18.2018.
[44] J.-Q. Zhang, S.-F. Huang, S.-T. Pang, M.-S. Wang, and S. Gao, "Synchronization in the uncoupled neuron system," *Chin. Phys. Lett.*, vol. 32, no. 12, Dec. 2015, Art. no. 120502, doi: 10.1088/0256-307x/32/12/120502.
[45] C. A. Sierra, "Recurrence in Lissajous curves and the visual representation of tuning systems," *Found. Sci.*, pp. 1–9, Oct. 2023, doi: 10.1007/s10699-023-09930-z.
[46] Xilinx Company (2023). *System Generator for DSP Tool*. Accessed: Nov. 10, 2023. [Online]. Available: www.xilinx.com
[47] Q. Xu, X. Chen, B. Chen, H. Wu, Z. Li, and H. Bao, "Dynamical analysis of an improved FitzHugh-nagumo neuron model with multiplier-free implementation," *Nonlinear Dyn.*, vol. 111, no. 9, pp. 8737–8749, May 2023, doi: 10.1007/s11071-023-08274-4.
[48] J. Cai, H. Bao, Q. Xu, Z. Hua, and B. Bao, "Smooth nonlinear fitting scheme for analog multiplierless implementation of Hindmarsh–Rose neuron model," *Nonlinear Dyn.*, vol. 104, no. 4, pp. 4379–4389, Jun. 2021, doi: 10.1007/s11071-021-06453-9.
[49] M. Heidarpur, A. Ahmadi, and N. Kandalaft, "A digital implementation of 2D Hindmarsh–Rose neuron," *Nonlinear Dyn.*, vol. 89, no. 3, pp. 2259–2272, Aug. 2017, doi: 10.1007/s11071-017-3584-0.
[50] M. Hayati, M. Nouri, D. Abbott, and S. Haghiri, "Digital multiplierless realization of two-coupled biological Hindmarsh–Rose neuron model," *IEEE Trans. Circuits Syst. II, Exp. Briefs*, vol. 63, no. 5, pp. 463–467, May 2016, doi: 10.1109/TCSII.2015.2505258.
[51] S. Gomar and A. Ahmadi, "Digital multiplierless implementation of biological adaptive-exponential neuron model," *IEEE Trans. Circuits Syst. I, Reg. Papers*, vol. 61, no. 4, pp. 1206–1219, Apr. 2014, doi: 10.1109/TCSI.2013.2286030.

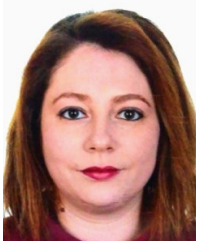

NIMET KORKMAZ received the B.S. degree in electrical and electronics engineering from Erciyes University, Kayseri, Turkey, in 2010, and the M.S. and Ph.D. degrees in electrical and electronics engineering from the Graduate School of Natural and Applied Sciences, Erciyes University, in 2012 and 2018, respectively. She was a Research Assistant with Erciyes University, until 2018. She is currently an Assistant Professor with the Department of Electrical and Electronics Engineering, Kayseri University. Her research interests include nonlinear systems, embedded systems, neural circuits and systems, central pattern generators, FPAA and FPGA-based analog, and digital circuit designs.